

# Journal of Biomedical Optics

[SPIEDigitalLibrary.org/jbo](http://SPIEDigitalLibrary.org/jbo)

## **Single fiber reflectance spectroscopy on cervical premalignancies: the potential for reduction of the number of unnecessary biopsies**

Sanaz Hariri Tabrizi  
S. Mahmoud Reza Aghamiri  
Farah Farzaneh  
Arjen Amelink  
Henricus J. C. M. Sterenberg

# Single fiber reflectance spectroscopy on cervical premalignancies: the potential for reduction of the number of unnecessary biopsies

Sanaz Hariri Tabrizi,<sup>a</sup> S. Mahmoud Reza Aghamiri,<sup>a</sup> Farah Farzaneh,<sup>b</sup> Arjen Amelink,<sup>c</sup> and Henricus J. C. M. Sterenborg<sup>c</sup>

<sup>a</sup>Shahid Beheshti University, Department of Radiation Medicine Engineering, Evin, Tehran, Iran

<sup>b</sup>Shahid Beheshti University of Medical Sciences, Gynecology Translational Research Center, Department of Obstetrics and Gynecology, Evin, Tehran, Iran

<sup>c</sup>Erasmus Medical Center, Center for Optical Diagnostics and Therapy, Department of Radiation Oncology, Rotterdam 3015 GE, The Netherlands

**Abstract.** We have assessed the value of single fiber reflectance (SFR) spectroscopy in prediction of cervical squamous intraepithelial lesions (SIL). SFR was used to measure reflected light from 32 patients undergoing standard colposcopy. Seven parameters extracted from the spectra in addition to two biographic parameters were compared in biopsy-confirmed SIL versus nonSIL. The significant parameters in the model were determined using stepwise logistic regression. The classification performance was evaluated by a leave-one-out cross-validation method and reported by receiver operating characteristic (ROC) curves. Light absorption properties and biographic characteristics of the patient contributed significantly to the accuracy of the model. Combining important parameters, the best retrospective sensitivity, specificity and area under the ROC curve for SIL sites versus nonSIL were 89%, 80% and 0.89%, respectively. SFR spectroscopy shows promise as a noninvasive, real-time method to guide the clinician in reducing the number of unnecessary biopsies. Discrimination of SIL from other abnormalities compares favorably with that obtained by fluorescence alone and by fluorescence combined with reflectance spectroscopy while the simplicity and low cost of the presented system are dominant. © 2013 Society of Photo-Optical Instrumentation Engineers (SPIE). [DOI: 10.1117/1.JBO.18.1.017002]

Keywords: precancer diagnosis; biomedical optics; single fiber reflectance spectroscopy; cervical intraepithelial neoplasia; cervical squamous intraepithelial lesions.

Paper 12588 received Sep. 5, 2012; revised manuscript received Nov. 13, 2012; accepted for publication Nov. 27, 2012; published online Jan. 4, 2013.

## 1 Introduction

Cervical cancer is the third most common cancer among women in the world. It is estimated that 12,170 new cases will be diagnosed in 2012, of which 35% will end with death.<sup>1</sup> Since 1950 when the Papanicolaou test (Pap smear) was introduced in the United States, both the incidence and the mortality rates of cervical cancer have decreased. This is due to the detection of pre-invasive and early stage of the disease using the Pap smear test followed by colposcopy. However, current screening and diagnostic protocol have some limitations including low sensitivity of the Pap smear test,<sup>2</sup> low sensitivity of the colposcopy,<sup>3</sup> and poor specificity of the colposcopy which often leads to needless biopsies.<sup>4</sup> Neither the Pap smear nor colposcopy-directed biopsy provides real-time diagnostic information. In order to decrease the referral times of the patient for treatment, “see and treat” protocols have been proposed. However, inaccuracies in Pap smear results and colposcopic impression often lead to over-treatment.<sup>5</sup>

In order to diagnose undetectable lesions and to reduce the number of unnecessary biopsies, substitute or adjunct methods with higher sensitivity and specificity in cervical intraepithelial neoplasia (CIN) detection are under investigation and

development. One of these methods is light spectroscopy. Since the late 20th century, many researchers have investigated the use of optical spectroscopy as an adjunct to the routine colposcopy to reduce the screening and surveillance costs and to improve detection of high grade squamous intraepithelial lesions (HGSIL) in the diagnostic and screening populations.<sup>6</sup>

Reflectance spectroscopy is a method that allows noninvasive determination of the scattering and absorption properties of a turbid medium, such as tissue. This information can be used to describe aspects of the tissue physiology (e.g., vascular oxygen saturation, blood volume fraction) and morphology (e.g., tissue, cell, organelle size and density).<sup>7</sup> One such method is single fiber reflectance (SFR) spectroscopy, which has the advantages of small probe size and simple device design.<sup>8</sup> This technique has the potential to assist clinicians in the selection of tissue extraction during standard biopsy procedures and is applicable in tissues such as lymph nodes.<sup>9</sup> In addition, the use of SFR has been studied in differentiating *ex vivo*<sup>10,11</sup> and *in vivo*<sup>12</sup> cancerous tissues from noncancerous tissues.

In this study the applicability of SFR in CIN detection has been examined. CIN is known as a precursor of cervical cancer. It is categorized to three levels named CIN I, II and III. The classification threshold for detection of premalignancies of the cervix varies according to different studies but many chose HGSIL (lump of CIN II and CIN III and worse) as the most

Address all correspondence to: Farah Farzaneh, Emam Hossein Hospital, Gynecology Translational Research Center, Department of Obstetrics and Gynecology, Nezam Abad Ave., Tehran, Iran. Tel: +98 21 77558081; Fax: +98 21 77557069; E-mail: F\_farzaneh@sbm.ac.ir or farahzaneh@yahoo.com

relevant.<sup>13</sup> Although HGSIL is more likely to progress to invasive carcinoma as compared with low grade lesions, the patients with CIN I pathology need to be followed up by HPV DNA testing at 12 months or cervical cytology at six months intervals.<sup>4</sup> Therefore, SIL (CIN I and worse) can be selected as a suitable threshold to guide the clinician in deciding to biopsy a lesion or not. The purpose of this study was to assess the SFR spectroscopy in detection of CIN I lesions and worse in patients undergoing standard colposcopic evaluation. The performance of this method is reported by receiver operating characteristic (ROC) curves using leave-one-out (LOO) cross-validation method. In addition, a new dataset is introduced which employs the colposcopically collateral normal site measurements. It can account for the biographic characteristics of the patients. The sensitivity and specificity of *in vivo* SFR measurements were reported on “per site” basis.

## 2 Materials and Methods

### 2.1 Instrumentation

Figure 1 shows a schematic of the SFR system setup used to measure reflected light from the cervical tissue. The single fiber probe contains a single optical fiber that both delivers light to the tissue and collects light remitted from the tissue. The optical fiber is 800  $\mu\text{m}$  in diameter (NA = 0.22) to interrogate epithelial and stroma layers of the cervical tissue. During measurement, photons travel from a tungsten halogen light source (AVALIGHT-HAL-S; Avantes; Eerbeek, the Netherlands) through one arm of a bifurcated fiber and through the single fiber, after which it exits into the sample. Reflected photons that are collected by the single fiber travel through the second arm of the bifurcated fiber and into the spectrophotometer (AVASPEC-2048-USB2; Avantes; Eerbeek, the Netherlands).<sup>14</sup> Specular reflections at the probe tip due to refractive index mismatch between the fiber and the sample are minimized by polishing the single fiber probe tip at an angle of 15-deg.<sup>15</sup> A calibration procedure was utilized to account for other internal reflections, variability in lamp-specific output, and in fiber-specific transmission properties. The calibration involves

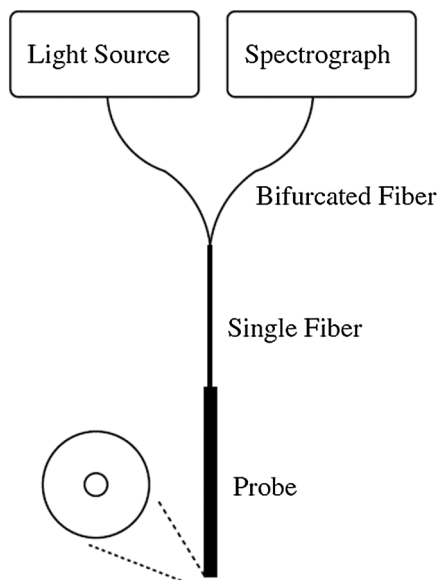


Fig. 1 Schematic of the single fiber reflectance (SFR) system setup.<sup>14</sup>

measurement of a high scattering solid phantom and measurement of water within a dark container.<sup>16</sup>

### 2.2 Single Fiber Reflectance Spectra

The SFR spectra were acquired using LabView software (Version 7.1; National Instruments) after putting the probe tip in contact with the tissue to be measured. Quantitative analysis of a measured SFR spectrum requires the use of an empirical model of both scattering and absorption properties of the tissue. The utilized model describes the wavelength-dependent collected light intensity in the absence of absorption ( $R_{\text{SF}}^0$ ) and applies a Modified Beer-Lambert law to that profile to account for absorption from tissue chromophores [Eq. (1)].<sup>17</sup>

$$R_{\text{SF}} = R_{\text{SF}}^0 e^{-\mu_a \langle L_{\text{SF}} \rangle}. \quad (1)$$

Here,  $\langle L_{\text{SF}} \rangle$  is the effective photon path length, which depends on the optical properties of the tissue and the fiber diameter as described below:<sup>15</sup>

$$\frac{\langle L_{\text{SF}} \rangle}{d_{\text{fiber}}} = \frac{1.54 \times C_{\text{PF}}}{(\mu'_s d_{\text{fiber}})^{0.18} (0.64 + (\mu_a d_{\text{fiber}})^{0.64})}, \quad (2)$$

where  $\mu'_s$  and  $\mu_a$  are the reduced scattering and absorption coefficients of the tissue, respectively. Also,  $C_{\text{PF}}$  describes the linear dependence of the scattering to the phase function which was estimated to be 0.944.<sup>17</sup> Other constant values in Eq. (2) were found using Monte Carlo simulations.<sup>15</sup>

A semi-empirical model was introduced for the reflected light intensity in the absence of absorption for SFR spectra [Eq. (3)].<sup>16</sup>

$$R_{\text{SF}}^0 = \eta_{\text{limit}} (1 + 1.55 e^{-6.82(\mu'_s d_{\text{fiber}})}) \times \left[ \frac{(\mu'_s d_{\text{fiber}})^{0.969}}{6.82 + (\mu'_s d_{\text{fiber}})^{0.969}} \right]. \quad (3)$$

Here,  $\eta_{\text{limit}}$  is the diffuse limit to the single fiber collection efficiency, which is 2.7% for a single fiber with NA = 0.22.<sup>17</sup> The constant values in Eq. (3) were estimated from Monte Carlo simulations by Kanick et al.<sup>17</sup> The absorption and scattering coefficients in Eqs. (1) through (3) are described below. Equation (4) models the reduced scattering coefficient which is a combination of Mie and Rayleigh scatterings and a function of the normalized wavelength to  $\lambda_0 = 800 \text{ nm}$ .<sup>18</sup>

$$\mu'_s = a_0 \left( \frac{\lambda}{\lambda_0} \right)^{a_1} + a_2 \left( \frac{\lambda}{\lambda_0} \right)^{-4}. \quad (4)$$

The  $a_0$ – $a_2$  parameters in Eq. (4) are the Mie scattering amplitude, Mie scattering slope and Rayleigh scattering amplitude, respectively. These parameters are found by fitting the data points in the spectra. The implemented absorbers in the model include hemoglobin<sup>19</sup> and beta-carotene,<sup>20</sup> which are the main absorbers in the cervix [Eq. (5)].<sup>18</sup>

$$\mu_a = a_3 \left[ \frac{1 - e^{-a_5 [\text{StO}_2 \times \mu_a^{\text{HbO}_2} + (1 - \text{StO}_2) \times \mu_a^{\text{Hb}}]}}{a_5 [\text{StO}_2 \times \mu_a^{\text{HbO}_2} + (1 - \text{StO}_2) \times \mu_a^{\text{Hb}}]} \right] \times [\text{StO}_2 \times \mu_a^{\text{HbO}_2} + (1 - \text{StO}_2) \times \mu_a^{\text{Hb}}] + a_6 \times \mu_a^{\text{Bcar}}. \quad (5)$$

Parameter  $a_3$  is the blood volume fraction,  $a_5$  is the average vessel diameter and  $a_6$  represents the concentration of beta-carotene.  $StO_2$  is the microvascular blood oxygenation which is defined as  $0.5 + [\text{Arctan}(a_4)]/\pi$  to apply an implicit boundary condition of  $0\% < StO_2 < 100\%$  in the fitting process.<sup>18</sup> Input spectrum  $\mu_a^{\text{Bcar}}$  is the specific absorption coefficient of beta-carotene<sup>21</sup> and  $\mu_a^{\text{HbO}_2}$  and  $\mu_a^{\text{Hb}}$  are the absorption coefficients of fully oxygenated and fully deoxygenated whole blood, respectively.<sup>22</sup>

Unknown parameters ( $a_0$ – $a_6$ ) in the model were fitted by minimizing the residual error between the spectrum and the model using Levenberg-Marquardt algorithm<sup>23</sup> that was scripted into LabView code. The fitted parameters consist of Mie scattering amplitude (Mie-amp), Mie scattering slope (Mie-sl), Rayleigh scattering amplitude (Ray-amp), blood volume fraction (BI-vol), blood oxygen saturation ( $StO_2$ ), average vessel diameter (Ves-diam) and beta-carotene concentration (B-car). The spectra were fitted in the 400 to 900 nm wavelength range.

### 2.3 In Vivo Measurements

The clinical *in vivo* study was conducted at Emam Hossein Medical and Educational Center and Taleghani General Hospital in Tehran from November 2011 to February 2012. The spectroscopic measurements were made on nonpregnant patients who were referred for colposcopy following an abnormal Pap smear, post-coital bleeding (PCB) and/or chronic cervicitis resistant to treatment. Before the experiment, each patient filled in the demographic questionnaire and signed an informed consent (with the approval of ethical committee of Shahid Beheshti University of Medical Sciences). The data were taken during a standard colposcopy procedure by the gynecological group. Before application of the probe, it was disinfected by 4% deconex® 53 PLUS (borer Co.) solution for at least half an hour. After application of 3% acetic acid to the cervix, the optical probe was placed in contact with the suspicious as well as colposcopically normal sites and reflected spectra were acquired. Generally all four quarters of the cervix were measured in each patient. In order to reduce the noise, five measurements were acquired from each probe position and averaged which took about 1 s. Afterwards, the average of the five spectra was fitted by the model. Based on ethical considerations, only the clinically abnormal appearing sites were biopsied. Special attention was given to obtain the biopsy from the same location as the measurement. Cervical tissue biopsies were fixed in formalin and submitted for histological examination. The tissue was classified into six categories: normal, cervicitis, human papillomavirus (HPV)-associated change, grade 1 cervical intraepithelial neoplasia (CIN I), grade 2 CIN (CIN II) and grade 3 CIN (CIN III). The latter two cases are combined as HGSIL while including the CIN I pathology in this set is known as squamous intraepithelial lesion (SIL). Example fits with corresponding residuals for four categories in our dataset is shown in Fig. 2.

### 2.4 Data Processing and Validation

The criteria to exclude data samples were:

1. large variation ( $>10\%$  average standard deviation in the 400 to 900 nm wavelength range) between five subsequent measurements on one site ( $n = 13$ )

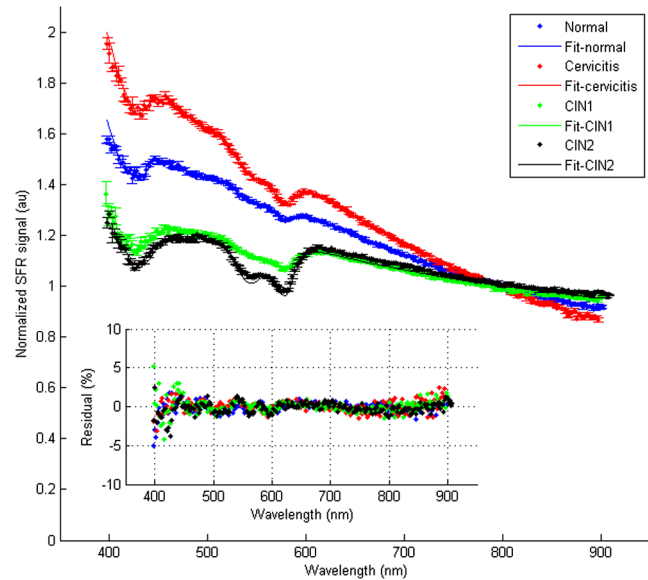


**Fig. 2** Typical normalized SFR spectra (dots with one standard deviation error bar of four pixels binned) for normal, cervicitis, CIN I and CIN II tissue types with the corresponding model fit (solid line). The percent residual is shown in the inner figure. For clarity, all the spectra are normalized to their value at 800 nm.

2. interference of the colposcope light in the measured spectra which was visible as a large dip in the 600 to 800 nm region ( $n = 4$ )
3. unsatisfactory biopsy specimen for histopathological evaluation ( $n = 11$ )
4. obtaining no biopsy ( $n = 4$ ).

Interference of the colposcope light was seen in the first few patients as zeroing the subtracted measured spectrum from the corresponding dark measurement. In order to overcome this problem, the next measurements were done while the light was undirected to the cervix, where the measurements were performed.

Thirty two patients ( $37 \pm 10$  years old) were evaluated which resulted in a total of 40 averaged evaluable spectra (Table 1). In this study SIL threshold was tested using multivariate logistic regression method. Classification of the two histopathology groups was carried out based on biopsy-confirmed spectra in order not to artificially increase the classifier accuracy.<sup>24</sup> The algorithm was validated using LOO cross-validation method and presented by ROC curves. Also, two-sided Wilcoxon rank sum test was used to test the hypothesis that the distribution of seven extracted spectroscopic parameters as well as two biographic variables [age and menopausal status (Mens) of the patient]<sup>19</sup> differed between the two categories. A  $p$ -value  $<0.05$  was considered to be significant.

It was found that normalizing the extracted parameters from each suspicious site by the corresponding value extracted from a clinically normal site from the same patient can improve the classification accuracy.<sup>24</sup> Therefore, in addition to seven spectroscopic parameters extracted from biopsy-confirmed sites, interaction of additional seven parameters from the colposcopically normal collateral sites were taken into account. The subtraction of each normal parameter from the corresponding

**Table 1** Characteristics of the measured sites.

Pathology	Number of sites	Number of patients <sup>a</sup>
Normal	6	4
Cervicitis	20	18
HPV effect	5	4
CIN I	5	3
CIN II	4	3
CIN III	0	0
Total	40	32

<sup>a</sup>The patients with more than one biopsy were assigned to the worst diagnostic group based on pathology result.

biopsy-confirmed one, resulted in a dataset called “SubParam”. Unsubtracted value of the parameters extracted from the suspicious site measurements constituted another dataset abbreviated as “AbsParam”. The classification algorithm and LOO validation method were applied to both absolute parameters (AbsParam) as well as subtracted parameter (SubParam) datasets.

### 3 Results

All measured suspicious lesions were biopsied and histologically classified. Table 1 summarizes the number of sites and patients measured for each pathology class. A Wilcoxon rank sum test was performed to determine if the mean values of nine

spectroscopic and biographic parameters differ between SIL sites versus all others (cutoff = CIN I). Table 2 shows the mean value and one standard deviation for each parameter. Both AbsParam and SubParam datasets were evaluated. Note that the values in SubParam column are the difference between corresponding parameters from a suspicious and a clinically normal collateral measurement. Among spectroscopic variables, only the vessel diameter is significantly different between the two pathologic groups for both AbsParam and SubParam datasets.

In order to draw the ROC curves, the relevant parameters for each dataset were selected using stepwise logistic regression. Stepwise regression is a systematic method for adding and removing terms from a multilinear model based on their statistical significance in a regression. The parameters were added to the model until the least difference was seen between the model and data points. Only the vessel diameter was found to be a significant parameter in both AbsParam and SubParam datasets.

Using the Ves-diam parameter, the probability of categorizing each measurement as an SIL was calculated by logistic regression method. The true positive rate (sensitivity) was drawn as a function of false positive rate (1-specificity) at various threshold settings to obtain the ROC curve. Figure 3 shows the ROC curves for AbsParam and SubParam datasets on a “per site” basis.

As shown in Fig. 3, with the perfect specificity of 100% (origin of the abscissa), the sensitivity of SIL detection is increased by usage of the SubParam dataset. The area under the ROC curve (AUC) for each category as well as the optimum sensitivity and specificity pair and contributed parameters in the model are shown in Table 3. The optimum sensitivity and specificity is defined as a point on the ROC curve with the shortest distance away from the point of perfect separation (100% sensitivity and 100% specificity).<sup>24</sup>

**Table 2** Wilcoxon rank sum test results for two sets of parameters with cutoff = CIN I.

Spectroscopic/biographic variables	AbsParam			SubParam		
	p value	Mean ± SD		p-value	Mean ± SD	
		NonSIL	SIL		NonSIL	SIL
Mie-amp (-)	0.092	0.43 ± 0.19	0.30 ± 0.11	0.364	-0.064 ± 0.19	-0.11 ± 0.21
Mie-sl (-)	0.771	-1.20 ± 0.37	-1.10 ± 0.41	0.559	-0.025 ± 0.40	-0.14 ± 0.41
Ray-amp (-)	0.627	0.0075 ± 0.014	0.007 ± 0.008	0.476	.0022 ± 0.014	-0.0028 ± 0.008
Bl-vol (-)	0.224	0.0034 ± 0.0036	0.0082 ± 0.016	0.559	0.00084 ± 0.0036	0.006 ± 0.017
StO2 (%)	0.559	73 ± 13	75 ± 13	0.517	2.1 ± 17.0	4.3 ± 16.0
Ves-diam (mm)	<b>0.0002</b>	<b>0.0060 ± 0.0074</b>	<b>0.021 ± 0.014</b>	<b>0.0096</b>	<b>0.00041 ± 0.007</b>	<b>0.011 ± 0.014</b>
B-car (μM)	0.120	6.5 ± 5.0	4.4 ± 3.7	0.120	1.1 ± 5.5	-0.86 ± 3.8
Age (years)	<b>0.011</b>	<b>40.0 ± 9.4</b>	<b>31.0 ± 9.4</b>	—	—	—
Mens (-)	0.255	0.52 ± 0.68	0.22 ± 0.44	—	—	—

Bold values in the table indicate the statistically significant ones ( $p < 0.05$ ).

Note that the age and menopausal parameters were eliminated in the SubParam category because of accounting them in the dataset itself (refer to Sec. 4.3).

SD: Standard deviation; SIL: Squamous intraepithelial lesion; AbsParam: Absolute parameter values extracted from biopsy-confirmed measurements; SubParam: Subtraction of normal collateral measurements from absolute parameter values extracted from biopsy-confirmed measurements.

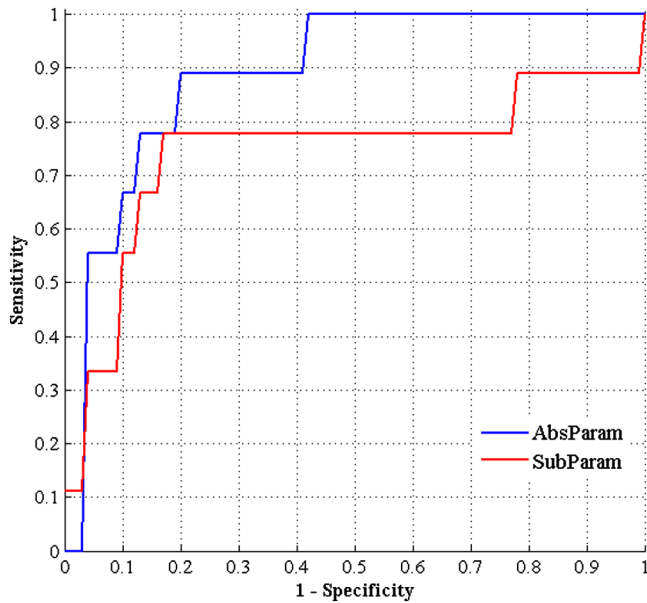


**Fig. 3** ROC curves for AbsParam and SubParam datasets with CIN I cutoff. (AbsParam: Absolute parameter values extracted from biopsy-confirmed measurements; SubParam: Subtraction of normal collateral measurements from absolute parameter values extracted from biopsy-confirmed measurements).

**Table 3** The area under the ROC curves (AUC) for AbsParam and SubParam datasets and the corresponding optimum sensitivity/specificity for SIL detection [with two standard deviations (95% CI)] are presented. The included variables in each category are shown, as well.

Dataset	AbsParam <sup>a</sup>	SubParam <sup>b</sup>
AUC	0.889 ± 0.014	0.745 ± 0.004
Sensitivity (%)	89 ± 0	78 ± 0
Specificity (%)	80 ± 3	83 ± 4
Included variables	Ves-diam	Ves-diam

<sup>a</sup>AbsParam: Absolute parameter values extracted from biopsy-confirmed measurements.

<sup>b</sup>SubParam: Subtraction of normal collateral measurements from absolute parameter values extracted from biopsy-confirmed measurements.

## 4 Discussion

### 4.1 System Accuracy

This study was conducted in order to evaluate the potential of SFR spectroscopy method to help the clinician in reducing the number of unnecessary biopsies in cervical tissue. Capability of the system in a pilot population was evaluated for distinguishing SIL measurements from the nonSIL. In comparison with some pilot studies in this field, our results are superior to some of them in differentiating SIL<sup>25-27</sup> from other tissue types on “per site” basis. When comparing the performance of SFR system with colposcopy alone, it should be noted that the performance of colposcopy varies considerably when the reports by Mitchell<sup>28</sup> and Alvarez<sup>29</sup> are compared. They reported a sensitivity of 96% and 53% per patient and specificity of 48% and 89% per patient, respectively. In either case, this system shows an intermediate performance.

Inclusion of clearly normal sites, as done in Refs. 19, 27, and 30, increases the specificity as determined on a “per site” basis because it is easier to differentiate HGSIL from truly normal tissue than HGSIL from metaplastic or inflamed tissue. In fact, the claimed sensitivity and specificity are directly influenced by the fraction of obvious lesions in the dataset. However, the clinician’s concern is to find the suitable biopsy location between a variety of suspicious sites and not an artificial increase in the performance.<sup>24</sup> Therefore, the inclusion of measurements from colposcopically normal sites was avoided in this study.

### 4.2 Effect of Spectroscopic Parameters

Unlike many other studies<sup>25,26,29</sup> the spectroscopic parameters used in this study have physical and biological interpretations. An advantage of using physically based measures rather than only a statistical analysis of the spectra is that the technique becomes less of a black box and the results may be presented to the medical staff in a more physiologically/medically relevant manner.<sup>19</sup> Moreover, the model incorporates prior knowledge on tissue optics that has been validated on more than 550 patients to date.<sup>7,9</sup>

As shown in Table 2, vessel diameter is a significant parameter in differentiating SIL from nonSIL and it increases with neoplasia progression. This finding is in accordance with increased neovascularity (and increased blood flow) with angiogenesis progression.<sup>27</sup> The important contribution of the vessel diameter in the model was confirmed by the stepwise logistic regression method.

In our study, weak contribution was found for some spectroscopic parameters including scattering properties of the medium and the beta-carotene concentration. Although many authors have found scattering properties of the diffuse reflectance spectra diagnostically useful, only the absorption portion of SFR spectra was found to be significant in this study. It may be due to different threshold used in this study rather than HGSIL used in most of other similar studies. Mourant et al.<sup>19</sup> found an increase in scattering with progression of neoplasia. Mirkovic et al.<sup>24</sup> found that only scattering coefficient at 700 nm has diagnostic importance but the small number of recruited patients in the study is a limitation for this result. However, Weber et al.<sup>31</sup> did not find significant difference between normal and neoplastic tissue by using the scattering property extracted from reflectance spectra.

### 4.3 Effect of Biographic Parameters

Several authors have addressed biographic variables in their data analysis.<sup>19,32</sup> Parturition trauma, oral contraceptive use and irregular menstruation lead to different cervical tissue consistency and quality. In addition, the different cycle of menstruation in each patient results in different levels of estrogen hormone which in turn, influences the cervical epithelial thickness.<sup>33</sup> SubParam dataset was used to reduce diversity due to intrinsic patient-to-patient variations associated with age, hormonal contraception, menopausal status, time-dependent effect of acetic acid application on scattering and absorption properties of the tissue,<sup>24</sup> variability in the probe application by the clinician and any probable interfering variable. Hence, using SubParam dataset, the biographic parameters of age and menopausal status were not included in the comparison between the two groups (Table 2).

Menopausal status did not contribute significantly in SFR measurements due to no post or peri-menopausal case in the SIL group of this study. However, age was found to be a contributing parameter (Table 2). Using SubParam dataset resulted in a mild increase in the  $p$ -values in comparison with the AbsParam dataset (Table 2). This reduction in the significance is due to addition of the uncertainty associated with the normal site measurements to the variance in the suspicious site measurements.

The optimum sensitivity for SubParam dataset was found to be less than AbsParam dataset while its specificity showed a slight improvement compared to AbsParam. However, the AUC of AbsParam was markedly more than SubParam (Table 3). This implies that while using the normally appearing measurements can improve the specificity and decreases the number of unnecessary biopsies, altogether it cannot outperform the classification done using only the biopsy-confirmed measurements. In other words, taking only biopsy-confirmed parameters (AbsParam) into account, the system performance will be acceptable. It results in less measurement time and less analysis task in a real-time workflow because there will be no need to a normal site measurement. Larger population with diverse physiologic and biographic situations is needed to confirm this finding.

#### 4.4 System Simplicity

Unlike other researches in which at least five optical fibers<sup>6</sup> were gathered in a probe to illuminate the tissue and collect the reflected light or the fluorescence spectra from it, the method introduced in this paper utilized only a single fiber. The small probe dimension and use of one optical fiber have the advantages of low cost, system simplicity and easier service and maintenance procedures. In addition, this system can help in evaluation of the endocervical canal that is a major limitation of visual inspection of the cervix with acetic acid and other existing screening devices.<sup>32</sup>

Many authors have used the fluorescence spectra with several emission wavelengths<sup>25,26</sup> or its combination with reflectance spectra<sup>31,32</sup> for CIN detection. As a result, huge systems have been produced one of which has been approved by food and drug administration (FDA).<sup>29</sup> However, fewer studies have been conducted to evaluate the CIN detection capability by reflectance spectroscopy alone using a white light source.<sup>6</sup> The present study showed good potential of reflectance spectroscopy using a very simple system incorporating only a white light source, a spectrophotometer and a single optical fiber in cervical tissue diagnosis. Also, very quick measurement of less than one second makes it a real-time tool as an adjunct to colposcopy routine in clinics.

## 5 Summary

The main goal of this work was to provide synchronous information regarding sites that should be biopsied in order to decrease the number of unnecessary biopsies. Another long-term goal of this study can be considered as conjunction of SFR measurement with colposcopy to facilitate one stop see-and-treat programs. The purpose of almost all the similar studies was to introduce a simple and cost effective system to developing countries with less availability of cervical screening program infrastructure. The system presented in this study, which was tested in one of these countries, is simple, inexpensive and has a high accuracy. Although a decrease in the classifier performance with increase in the study sample size is likely,<sup>31</sup> the

current preliminary results are encouraging enough to test the system on a larger population, which is currently being done.

## Acknowledgments

This work was funded in part by the Ministry of Science, Research and Technology of Iran. We cordially acknowledge the collaboration of the gynecological department of Emam Hosseini Medical and Educational Center including: Drs. M.S. Hosseini, M. Arab, Z. Vahedpour Fard, F. Athar, A. Fazel, N. Safaiee, T. Ghasemi, N. Kazemi, F. Omidifar, K. Samadi and A. Shouman. We should also like to thank all the patients who participated in this study.

## References

1. N. Howlader et al., Eds. *SEER Cancer Statistics Review, 1975–2009* (Vintage 2009 Populations), National Cancer Institute, Bethesda, MD, [http://seer.cancer.gov/csr/1975\\_2009\\_pops09/](http://seer.cancer.gov/csr/1975_2009_pops09/) (2012).
2. ASCUS-LSIL Triage Study (ALTS) Group, "A randomized trial on the management of low-grade squamous intraepithelial lesion cytology interpretations," *Am. J. Obstet. Gynecol.* **188**(6), 1393–1400 (2003).
3. R. Pretorius et al., "Colposcopically directed biopsy, random cervical biopsy, and endocervical curettage in the diagnosis of cervical intraepithelial neoplasia II or worse," *Am. J. Obstet. Gynecol.* **191**(2), 430–434 (2004).
4. R. Guido et al., "Postcolposcopy management strategies for women referred with low-grade squamous intraepithelial lesions or human papillomavirus DNA-positive atypical squamous cells of undetermined significance: a two-year prospective study," *Am. J. Obstet. Gynecol.* **188**(6), 1401–1405 (2003).
5. L. Dainty et al., "Controversial topics in abnormal cervical cytology: see and treat," *Clin. Obstet. Gynecol.* **48**(1), 193–201 (2005).
6. S. Hariri Tabrizi et al., "The use of optical spectroscopy for *in vivo* detection of cervical pre-cancer," *Laser. Med. Sci.*, Under review (2012).
7. A. Amelink et al., "Non-invasive measurement of the morphology and physiology of oral mucosa by use of optical spectroscopy," *Oral Oncol.* **44**(1), 65–71 (2008).
8. M. Canpolat and J. R. Mourant, "Particle size analysis of turbid media with a single optical fiber in contact with the medium to deliver and detect white light," *Appl. Opt.* **40**(22), 3792–3799 (2001).
9. S. C. Kanick et al., "Characterization of mediastinal lymph node physiology *in vivo* by optical spectroscopy during endoscopic ultrasound-guided fine needle aspiration," *J. Thorac. Oncol.* **5**(7), 981–987 (2010).
10. M. Canpolat et al., "Differentiation of melanoma from non-cancerous tissue in an animal model using elastic light single-scattering spectroscopy," *Technol. Cancer Res. Treat.* **7**(3), 235–240 (2008).
11. M. Canpolat et al., "Intra-operative brain tumor detection using elastic light single-scattering spectroscopy: a feasibility study," *J. Biomed. Opt.* **14**(5), 054021 (2009).
12. M. Canpolat et al., "Diagnosis and demarcation of skin malignancy using elastic light single-scattering spectroscopy: a pilot study," *Dermatol. Surg.* **38**(2), 215–223 (2012).
13. M. Cardenas-Turan et al., "The clinical effectiveness of optical spectroscopy for the *in vivo* diagnosis of cervical intraepithelial neoplasia: where are we?" *Gynecol. Oncol.* **107**(Suppl. 1), S138–S146 (2007).
14. S. C. Kanick, H. J. C. M. Sterenborg, and A. Amelink, "Empirical model of the photon path length for a single fiber reflectance spectroscopy device," *Opt. Exp.* **17**(2), 860–871 (2009).
15. S. C. Kanick et al., "Monte Carlo analysis of single fiber reflectance spectroscopy: photon path length and sampling depth," *Phys. Med. Biol.* **54**(22), 6991–7008 (2009).
16. S. Kanick et al., "Measurement of the reduced scattering coefficient of turbid media using single fiber reflectance spectroscopy: fiber diameter and phase function dependence," *Biomed. Opt. Express* **2**(1), 1687–1702 (2011).
17. S. C. Kanick et al., "Method to quantitate absorption coefficients from single fiber reflectance spectra without knowledge of the scattering properties," *Opt. Lett.* **36**(15), 2791–2793 (2011).

18. A. Amelink, D. Robinson, and H. J. C. M. Sterenborg, "Confidence intervals on fit parameters derived from optical reflectance spectroscopy measurements," *J. Biomed. Opt.* **13**(5), 054044 (2008).
19. J. Mourant et al., "In vivo light scattering measurements for detection of precancerous conditions of the cervix," *Gynecol. Oncol.* **105**, 439–445 (2007).
20. P. Palan et al., "Beta-carotene levels in exfoliated cervicovaginal epithelial cells in cervical intraepithelial neoplasia and cervical cancer," *Am. J. Obstet. Gynecol.* **167**(6), 1899–1903 (1992).
21. S. W. van de Poll, "Raman spectroscopy of atherosclerosis," Ph.D. Thesis, p. 123, University of Leiden, Leiden, Netherlands (2003).
22. A. Amelink, T. Christiaanse, and H. J. C. M. Sterenborg, "Effect of hemoglobin extinction spectra on optical spectroscopic measurements of blood oxygen saturation," *Opt. Lett.* **34**(10), 1525–1527 (2009).
23. D. Marquardt, "An algorithm for least-squares estimation of nonlinear parameters," *SIAM J. Appl. Math.* **11**(2), 431–444 (1963).
24. J. Mirkovic et al., "Detecting high-grade squamous intraepithelial lesions in the cervix with quantitative spectroscopy and per-patient normalization," *Biomed. Opt. Express* **2**(10), 2917–2925 (2011).
25. M. F. Mitchell et al., "Fluorescence spectroscopy for diagnosis of squamous intraepithelial lesions of the cervix," *Obstet. Gynecol.* **93**(3), 462–470 (1999).
26. N. Ramanujam et al., "Development of a multivariate statistical algorithm to analyze human cervical tissue fluorescence spectra acquired in vivo," *Lasers Surg. Med.* **19**(1), 46–62 (1996).
27. J. R. Mourant et al., "In vivo light scattering for the detection of cancerous and precancerous lesions of the cervix," *Appl. Opt.* **48**(10), D26–D35 (2009).
28. M. Mitchell et al., "Colposcopy for the diagnosis of squamous intraepithelial lesions: a meta-analysis," *Obstet. Gynecol.* **91**(4), 626–631 (1998).
29. R. Alvarez, T. Wright, and O. D. Group, "Effective cervical neoplasia detection with a novel optical detection system: a randomized trial," *Gynecol. Oncol.* **104**(2), 281–289 (2007).
30. I. Georgakoudi et al., "Trimodal spectroscopy for the detection and characterization of cervical precancers in vivo," *Am. J. Obstet. Gynecol.* **186**(3), 374–382 (2002).
31. C. R. Weber et al., "Model-based analysis of reflectance and fluorescence spectra for in vivo detection of cervical dysplasia and cancer," *J. Biomed. Opt.* **13**(6), 064016 (2008).
32. S. B. Cantor et al., "Accuracy of optical spectroscopy for the detection of cervical intraepithelial neoplasia: testing a device as an adjunct to colposcopy," *Int. J. Cancer* **128**(5), 1151–1168 (2011).
33. C. E. Wood, "Morphologic and immunohistochemical features of the cynomolgus macaque cervix," *Toxicol. Pathol.* **36**(7S), 119S–129S (2008).